



City Research Online

## City, University of London Institutional Repository

---

**Citation:** Yan, D., Kovacevic, A. & Tang, Q. (2017). Numerical investigation of flow characteristics in twin-screw pump under cavitating conditions. IOP Conference Series: Materials Science and Engineering, 232(1), 012026. doi: 10.1088/1757-899x/232/1/012026

This is the published version of the paper.

This version of the publication may differ from the final published version.

---

**Permanent repository link:** <https://openaccess.city.ac.uk/id/eprint/18564/>

**Link to published version:** <https://doi.org/10.1088/1757-899x/232/1/012026>

**Copyright:** City Research Online aims to make research outputs of City, University of London available to a wider audience. Copyright and Moral Rights remain with the author(s) and/or copyright holders. URLs from City Research Online may be freely distributed and linked to.

**Reuse:** Copies of full items can be used for personal research or study, educational, or not-for-profit purposes without prior permission or charge. Provided that the authors, title and full bibliographic details are credited, a hyperlink and/or URL is given for the original metadata page and the content is not changed in any way.

---

---

---

City Research Online:

<http://openaccess.city.ac.uk/>

[publications@city.ac.uk](mailto:publications@city.ac.uk)

---

PAPER • OPEN ACCESS

## Numerical investigation of flow characteristics in twin-screw pump under cavitating conditions

To cite this article: D Yan *et al* 2017 *IOP Conf. Ser.: Mater. Sci. Eng.* **232** 012026

View the [article online](#) for updates and enhancements.

### Related content

- [Suitability research on the cavitation model and numerical simulation of the unsteady pulsed cavitation jet flow](#)  
S Y Chen, X F Yu, D Y Luan *et al.*
- [Analysis of flow characteristics of a cam rotor pump](#)  
Y Y Liu, T C Miao, D Z Wu *et al.*
- [Investigation on cavitation for hump characteristics of a pump turbine in pump mode](#)  
D Y Li, H J Wang, G M Xiang *et al.*

# Numerical investigation of flow characteristics in twin-screw pump under cavitating conditions

D Yan<sup>1,2</sup>, A Kovacevic<sup>2</sup>, Q Tang<sup>1</sup>, S Rane<sup>2</sup>

<sup>1</sup>State Key Laboratory of Mechanical Transmission, Chongqing University, 400044, China;

<sup>2</sup>Centre for Compressor Technology, City University of London, EC1V0HB, UK

**Abstract.** In order to investigate the flow characteristics and the formation process of cavitation in twin-screw pumps, three-dimensional CFD (Computational Fluid Dynamics) numerical analysis has been carried out. A conformal structured moving mesh generated by an in-house code SCORG was applied for the rotor domain. The VOF (Volume of Fluid) Method has been adopted for dealing with the liquid-gas two-phase flow, while the bubble dynamics was handled by a homogenous cavitation model. By changing the rotation speed and discharge pressure, the intensity, distribution area and variation of cavitation at different rotor angle were obtained. The effects of rotation speed and discharge pressure on cavitation characteristics have been analysed. Calculation results with cavitation model are compared with the results without cavitation and the experimentally obtained values. The influence of cavitation on the performance of a screw pump in terms of the mass flow rate, pressure distribution, rotor torque and the shaft power have been analysed and discussed.

## 1. Introduction

Twin screw pumps are positive displacement machines widely used in petrochemical, shipping, energy and food industries due to their reliability, self-priming capability and excellent performance in single phase or multiphase operation. Typical arrangement of a twin screw liquid pump is given in Figure 1, showing rotors synchronised by timing gears and enclosed in the casing.



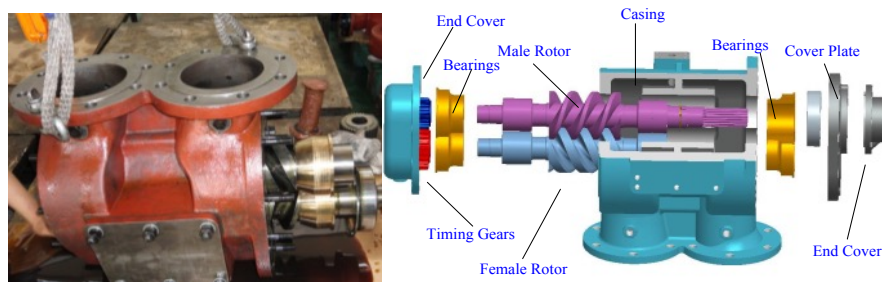


**Figure 1.** Structure and components of twin-screw pump

With the trend of increasing rotational speed, delivery pressure and power in screw pumps, the cavitation becomes a phenomenon unavoidable in such kinds of machines. Nowadays, the research of cavitation is mainly focused on centrifugal pumps, hydrofoils, propellers and hydraulic valves, etc.[1]. The lobes of a positive displacement screw pump are much thicker than in turbo machines, while the clearances of screw pumps are much smaller than in dynamic pumps. Positive displacement machines also rotate slower than equivalent size dynamic machines. Therefore such machines are less sensitive to cavitation, and usually no obvious cavitation erosion is observed on screw rotor surfaces. For that reason less attention is paid in the literature to the cavitation in screw pumps [2]. However, during the rotation of screw rotors, cavitation develops through initiation, growth and collapse of bubbles, which will directly influence the performance of a screw pump, such as increasing vibration and noise, eroding surfaces of rotors and casing wall, lowering the volumetric efficiency, and so on [3]. Therefore, in order to improve the performance and stability of screw pump and expand its application fields, cavitation cannot be ignored.

In this paper, the unique grid generation software SCORG is used for grid generation of a structured moving mesh around screw pump rotors [4]. The mesh for stationary domains such as ports and pipes is generated by use of a commercial grid generator built into the CCM (Computational Continuum Mechanics) solver STAR-CCM+ [5]. Handling of the mesh generated by SCORG in STAR-CCM+ solver is managed by use of the UDF made specially for handling conformal rotor mesh and it will be described later in the paper. This method has been validated by experiment in single-phase CFD modelling of screw pump [6][7].

The aim of this paper is to study the flow characteristics of twin-screw pumps under cavitating conditions. Based on the structured moving mesh, full CFD simulations with and without cavitation have been carried out and will be explained in detail in this paper. The real-time mass flow rate, rotor torque, pressure distribution, velocity field, power consumption were obtained. In cavitation modelling, Volume of Fluid (VOF) model [8] was applied for dealing with the liquid-gas two-phase flow. The Sauer-Schnerr model was used for modelling bubble dynamics. By changing rotation speed and discharge pressure separately, the accordingly variation of cavitation was acquired. The influence of cavitation on performance of a screw pump was analysed and discussed.

## 2. Mathematical Model

Positive displacement screw pumps operate on the basis of changing the size and position of a working domain which consequently causes change in the pressure of the working domain thereby transporting the fluid. To calculate performance of a screw pump, quantities such as mass, momentum, energy etc. need to be modelled. The governing equations required for the solution a closely coupled, time

dependent set of partial differential equations (PDE's) and often employ a Finite Volume Method (FVM) to be solved [9][10].

### 2.1. Governing Equations

The cavitating flow can be treated as a homogeneous mixture of vapour, air and liquid, in which vapour and air are gas. So it is liquid-gas two-phase flow. VOF model considers a single effective fluid whose properties vary according to volume fraction of individual fluids:

$$\alpha_i = \frac{V_i}{V} \quad (1)$$

The mass conservation equation for fluid  $i$  reads:

$$\frac{\partial(\alpha_i \rho_i)}{\partial t} + \nabla \cdot (\alpha_i \rho_i \mathbf{v}) = \rho_i S_{\alpha_i} \quad (2)$$

It can be rearranged into an equation in integral form:

$$\frac{\partial}{\partial t} \int_V \alpha_i dV + \int_S \alpha_i \mathbf{v} \cdot \mathbf{n} dS = \int_V \left( S_{\alpha_i} - \frac{\alpha_i D_{\rho_i}}{\rho_i Dt} \right) dV \quad (3)$$

where  $S_{\alpha_i}$  is the source of the phase  $i$

This equation is used to compute the transport of volume fraction  $\alpha_i$

The mass conservation equation for the effective fluid is obtained by summing up all component equations and using the condition:

$$\sum_i \alpha_i = 1 \quad (4)$$

The integral form of mass conservation equation (used to compute pressure correction) reads:

$$\int_S \mathbf{v} \cdot \mathbf{n} dS = \sum_i \int_V \left( S_{\alpha_i} - \frac{\alpha_i D_{\rho_i}}{\rho_i Dt} \right) dV \quad (5)$$

The properties of effective fluid are computed according to volume fractions:

$$\rho = \sum_i \alpha_i \rho_i \quad (6)$$

The VOF model description assumes that all immiscible fluid phases present in a control volume share velocity, pressure, and temperature fields. Therefore, the same set of basic governing equations describing momentum, mass, and energy transport as in a single-phase flow is solved.

The equations are solved for an equivalent fluid whose physical properties are calculated as functions of the physical properties of its constituent phases and their volume fractions.

### 2.2. Cavitation Model

The cavitation model describes the growth of bubbles which includes the phase change between liquid and its vapour. In this calculation, a homogenous distribution of bubble seeds in the liquid was applied. Based on the Rayleigh-Plesset equation [11], the vapour volume fraction can be calculated as follows:

$$\alpha_v = \frac{V_v}{V_l + V_v} = \frac{n_0 V_l \frac{4}{3} \pi R^3}{V_l + n_0 V_l \frac{4}{3} \pi R^3} = \frac{n_0 \frac{4}{3} \pi R^3}{1 + n_0 \frac{4}{3} \pi R^3} \quad (7)$$

The bubble growth rate reads:

$$\dot{R} = \frac{dR}{dt} = \sqrt{\frac{2P_B - P_\infty}{3\rho_l}} \quad (8)$$

then the vapour production rate reads:

$$\frac{d\alpha}{dt} = (1 - \alpha) \frac{4\pi n_0 R^2}{1 + \frac{4}{3}n_0\pi R^3} \dot{R} \quad (9)$$

The continuity equation reads:

$$\nabla \cdot \mathbf{v} = -\frac{1}{\rho} \left( \frac{\partial \rho}{\partial t} + \mathbf{v} \cdot \nabla \rho \right) = -\frac{1}{\rho} \frac{d\rho}{dt} = \frac{\rho_l - \rho_v}{\rho} \frac{d\alpha}{dt} \quad (10)$$

Then the transport equation reads:

$$\frac{d\alpha}{dt} + \nabla \cdot (\alpha \mathbf{v}) = \frac{d\alpha}{dt} + \alpha \nabla \cdot \mathbf{v} = \frac{(1 - \alpha)\rho_l}{(1 - \alpha)\rho_l + \alpha\rho_v} \frac{n_0}{1 + n_0 \frac{4}{3}\pi R^3} \frac{d}{dt} \left( \frac{4}{3}\pi R^3 \right) \quad (11)$$

### 3. Setup for Calculation of the Screw Pump

The screw pump used for this study shown in Figure 1 is a twin-screw pump with a 2/3 lobe arrangement and A-type profile rotors. The operating speed of the male rotor changes from 630 to 2100 rpm while keeping the discharge pressure as 0.85 MPa. By controlling the discharge valve, the discharge pressure varies from 0.35 to 0.85 MPa while keeping rotation speed of the male rotor at 2100 rpm. The male and the female rotors have 140.00 mm diameter and the centre distance of 105.00 mm. The length of the rotors is 200.00 mm and the male rotor has a wrap angle of 590.0°.

#### 3.1. Grid Generation

Grid generation is a process of discretising a working domain of the screw pump in control volumes for which a solution of local fluid properties is to be found. It may be numerical, analytical or variational [12]. The results obtained in this research work used grids generated by analytical grid generation. Applying the principles of analytical grid generation through transfinite interpolation with adaptive meshing, the authors have derived a general, fast and reliable algorithm for automatic numerical mapping of arbitrary twin screw machine geometry built into an in-house grid generation code SCORG[13][14].

The rotor profile of the screw pump is shown in Figure 2. Table 1 shows the geometry parameters of rotors. The numerical grid for the working fluid domain between two rotors is shown as Figure 3.

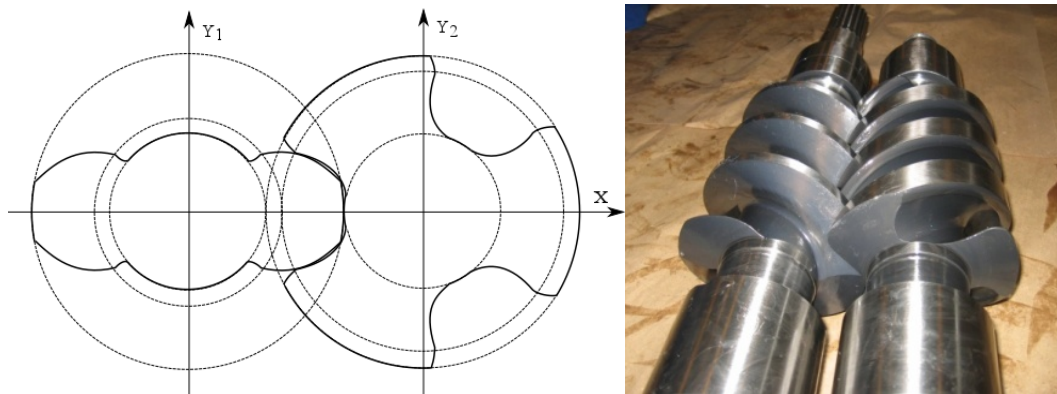


**Figure 2.** A-type tooth profile used in this paper

**Table 1.** Geometry parameters of screw rotors used in study

	Number of Lobes	Pitch Radius ( <i>mm</i> )	Root Radius ( <i>mm</i> )	Tip Radius ( <i>mm</i> )
Male Rotor	2	42	35	70
Female Rotor	3	63	35	70
Centre distance		105 <i>mm</i>		
Thread pitch		61 <i>mm</i>		
Radial clearance		0.24 <i>mm</i>		
Inter-lobe clearance		0.12 <i>mm</i>		



**Figure 3.** Grids in the fluid domain(left) in cross section of rotors; middle) on the rotor surface; right) polyhedral mesh of suction and discharge ports

Polyhedral mesh of the inlet port and outlet port is generated using STAR-CCM+ grid generator as shown in Figure 3(right). The grid independency study for this calculation model has already been performed in another publication [6]. A numerical mesh used in this study comprises 1068864 cells of which 775180 cells represent the fluid domain between the rotors while 293684 cells represent the two ports.

### 3.2. Numerical Methods

The Star-CCM+ pressure-based solver is used for the calculation of screw pump. In order to solve the pressure-velocity coupling, the implicit unsteady segregated flow scheme has been applied. The second-

order upwind discretization scheme is applied. Gauss-Seidel node is used for the relaxation scheme which provides better convergence by iteratively correcting (relaxing) the linear equation during multigrid cycling.

The main rotor rotates  $2.4^\circ$  per step. The mesh is updated before commencing solution for each time step. The time-step is defined as follows:

$$\Delta t = \frac{DPTS}{6 \cdot RPM} \quad (12)$$

whereby,  $DPTS$  is the degree per time step,  $RPM$  is the rotation speed of male rotor.

When the  $DPTS$  is not small enough, it will make the simulation run with a relatively large time-step which may cause the divergence of calculation. Here,  $\Delta t$  is inversely proportional to  $RPM$ , which means that the mesh has to be changed for different  $RPM$  in order to keep the ratio of time and spatial step constant. It's not always essential to keep the ratio constant but it is limited by Courant stability condition.

The k- $\epsilon$  turbulence model is adopted in the calculation. Stagnation inlet and pressure outlet are used respectively for the inlet and outlet boundaries. The pressure of the inlet port is 0 Pa. The discharge pressure ranges from 0.35 to 0.85MPa while the rotation speed of the male rotor ranges from 630 to 2100 rpm. The initial pressure and initial velocity are 0 Pa and 0 m/s respectively. The turbulence intensity is 1% and the turbulence viscosity ratio is 10.

#### 4. Numerical Results

The calculations were carried out in a computer powered by 4 Intel 3.00 GHz processors and 8 GB memory. Screw pump rotation was simulated by means of 75 time steps for one interlobe rotation, which was equivalent to 150 time steps for one full rotation of the male rotor. The time step length was synchronised with a rotation speed of 630 to 2100 rpm. An error reduction of 4 orders of magnitude was required, and achieved in 30 inner iterations at each time step. The overall performance parameters such as chamber pressure, velocity distribution, rotor torque, mass flow rate and shaft power were then calculated.

##### 4.1. Cavitation under Different Boundary Conditions

The start-up process of a screw pump is highly unsteady leading to the large area of cavitation in the pump chamber in a short period of time. As time progresses, the flow field gradually reaches a steady state condition when the domain in which fluid cavitates becomes reduced and repeats periodically. Figure 4 shows the volume fraction of vapour observed in the working domain as the function of the rotation angle under different rotation speed and different discharge pressure. It can be observed from Figure 4(left) it can be observed that, when cavitation stabilized, the volume fraction of cavitation and its fluctuation amplitude repeat and are higher for higher rotation speeds.

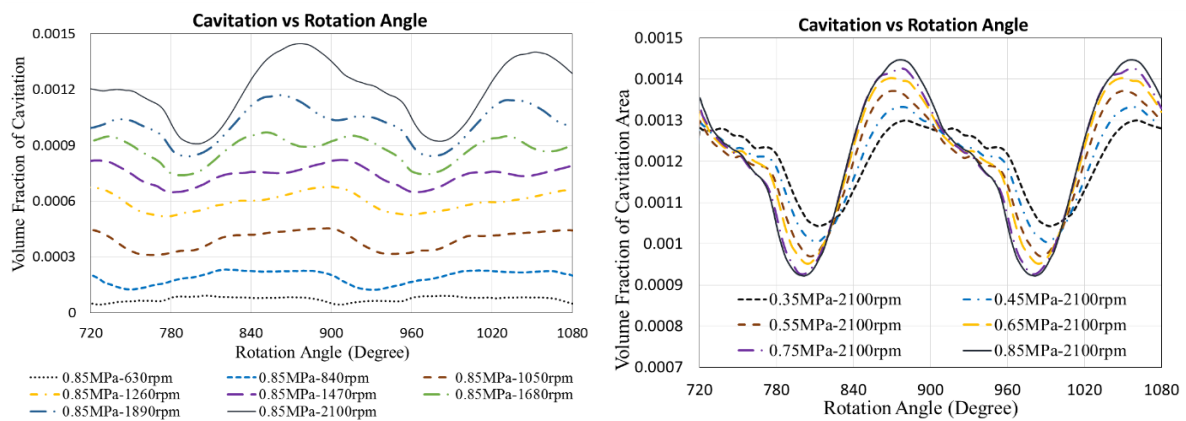


**Figure 4.** Cavitation changes at different rotation angles: (left) under different rotation speeds; (right) under different discharge pressure

Figure 4 (right) shows the changes of the maximum volume fraction of vapour with the constant rotation speed at different discharge pressures. When the pump reached steady state conditions, the average volume fraction of cavitation nearly remains the same under different discharge pressure, while the amplitude of volume fraction remains higher for higher pressure difference between the suction and discharge pressures. Compared with Figure 4(left), it can be observed that the effect of the discharge pressure on cavitation is not as significant as in the case of increased rotation speed.

Figure 5 shows the location of the cavitation area at different rotor angle when the screw pump reaches a relatively stable state at 2100rpm and 0.85MPa. The increased volume fraction of vapour is mainly located in the radial and inter-lobe clearances near the suction port, and its value changes periodically with the rotation of the rotors.

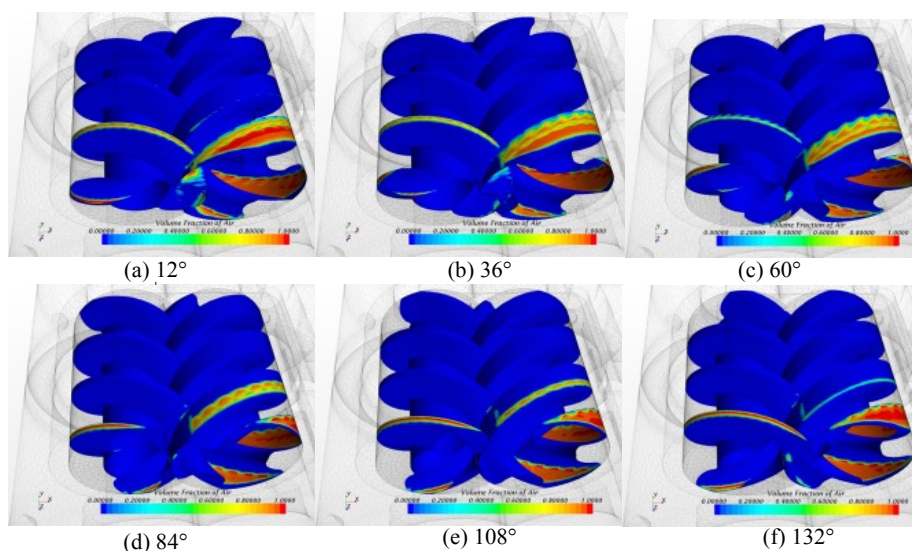


**Figure 5.** Cavitation distribution at 2100rpm and 0.85MPa under different rotation angle

When the screw pump reaches a relatively stable state at 630rpm and 0.85MPa. The area where fluid cavitates is the same as for the higher speed but its amplitude is much smaller especially on the female rotor. When comparing with values in Figure 5 for speed of 2100 rpm, it can be concluded that the

cavitation weakens with the decrease of rotation speed.

To investigate what will happen at much higher speeds, a calculation is performed for 4 times the maximum speed of the liquid pump, in this case 8400 rpm. In such case, cavitation is not limited just to the clearance area, it extends to the entire chamber and also will spread to other chambers in the axial direction from the suction. It would take much longer for cavitation to reduce. The mean value of the volume fraction of vapour and its amplitude would both increase compared to lower speeds shown in previous figures.

From the analysis above, it can be concluded that by controlling the rotation speed to a reasonable range, cavitation and its influence in screw pumps can be limited without the need to change the structure of the pumps. However, when designing high-speed screw pump, the inside structure of the pump needs to be designed carefully to reduce cavitation.

#### 4.2. Mass Flow Rate and Rotor Torque

In order to investigate effects of cavitation on the flow through the pump, two separate calculations were performed at 2100rpm and 0.85MPa discharge pressure, one without cavitation and another which includes modelling of the cavitation.

Figure 6(left) shows the calculated instantaneous mass flow rate of the screw pump with and without cavitation at 2100rpm and 0.85MPa. It can be seen from the comparison that the mass flow pulsations with cavitation included in prediction model are larger than that without cavitation, the fluctuation amplitude without cavitation is 0.62kg/s while under cavitation it is 1.03kg/s. The averaged mass flow rate under cavitation is similar to that without cavitation.

Figure 6(right) shows the rotor torque of screw pump with and without cavitation at 2100rpm and 0.85MPa. The periods of torque fluctuations with and without cavitation are the same. Cavitation brings a slightly increased amplitude of torque value. For the male rotor, the peak-to-peak amplitude of torque without cavitation is 11.83N-m, while which increases to 18.43N-m when with cavitation. The averaged torque of male rotor with and without cavitation are the same, while cavitation causes an increase of 3.17N-m which is 26.04% in averaged female rotor torque.

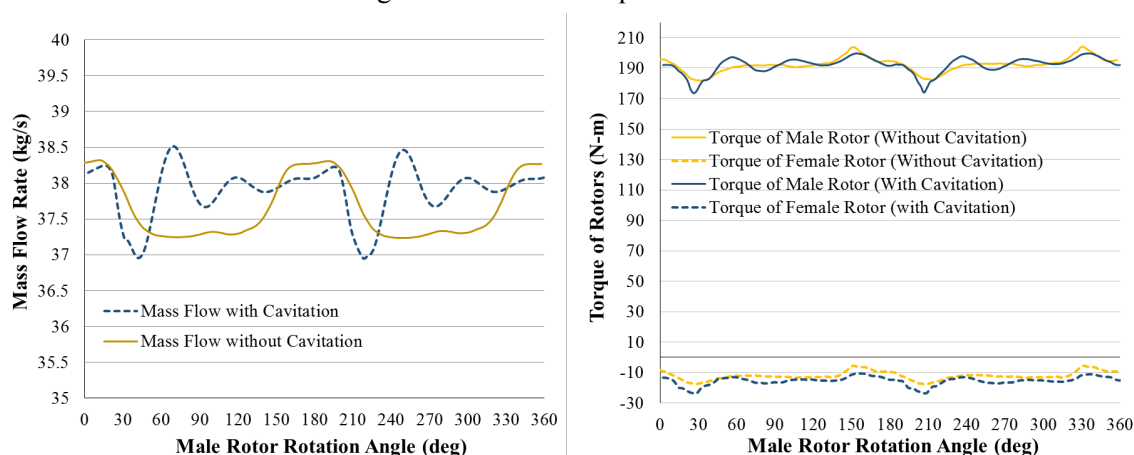


**Figure 6.** (left) Mass flow rate; (right) Rotor torque with and without cavitation under different rotation angle

## 5. Comparison with experiment and discussion

An experiment has been carried out to validate the calculation[6]. The working medium used in the experiment is CD40 lubricating oil. The density is  $889\text{kg/m}^3$  and the dynamic viscosity is  $5.25 \times 10^{-2}\text{Pa}\cdot\text{S}$ . The temperature of oil is  $50$  to  $70^\circ\text{C}$ . The nominal interlobe clearance (between two rotors) is  $0.12\text{ mm}$ , the nominal radial clearance (between rotor and casing) is  $0.24\text{ mm}$ .

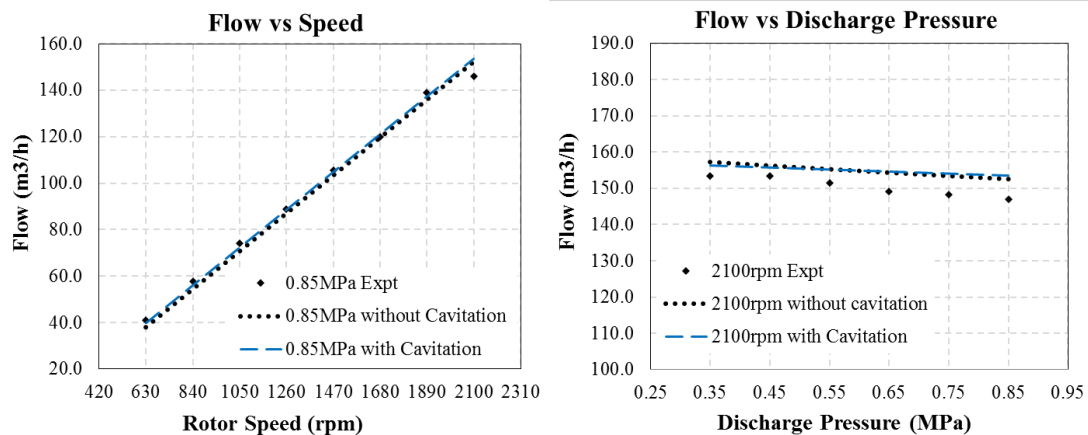


**Figure 7.** Flow rate: (left) variable rotational speed; (right) variable discharge pressure

Figure 7(left) shows the flow rate of cavitation and non-cavitation condition with the variation of rotation speed and (under constant discharge pressure  $0.85\text{MPa}$ ). By comparison, it can be found that with cavitation the flow rate is  $4.90\%$  higher than that without cavitation.

From the distribution of cavitation in Figure 5, it can be seen that under a relatively low rotation speed cavitation mainly appeared in clearance area. Clearance cavitation leads to a decrease of flow rate through clearances, which means smaller leakage rate. It is observed by analysing modelling results that forming of the vapour in clearances effects sealing and it brings a slightly increased volumetric efficiency of a screw pump.

Figure 7(right) shows the flow rate of cavitation and non-cavitation condition with the variation of discharge pressure and (under constant rotation speed  $2100\text{rpm}$ ). It can be found that the flow rates of both are very close. With the increase of discharge pressure, the flow rate under cavitation gradually exceeds that without cavitation in a small degree.

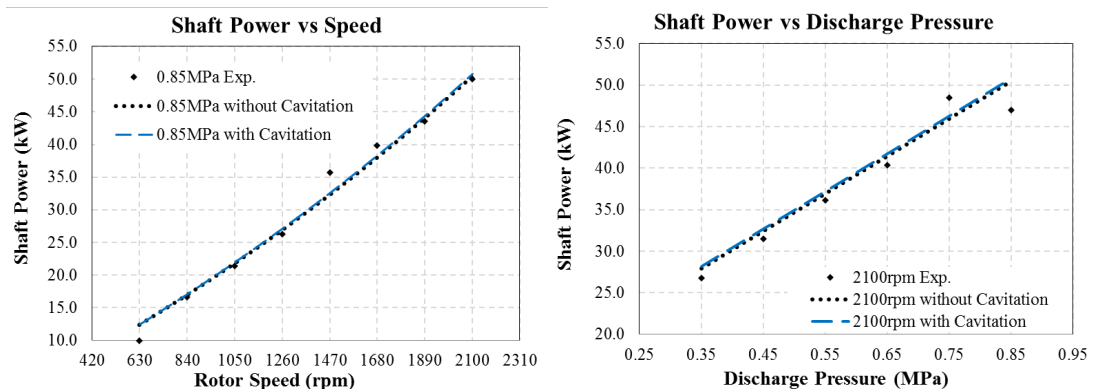


**Figure 8.** Shaft power: (left) variable rotational speed; (right) variable discharge pressure

Figure 8(left, right) shows the shaft power of screw pump under cavitation and non-cavitation with the

variation of rotation speed and discharge pressure. It can be found that cavitation and non-cavitation have a very close shaft power while cavitation brings a slightly increase of 1.21% in shaft power. The main reason caused higher power consumption is that cavitation influenced the pressure distribution in chamber and brought fluctuation and increase in rotor torque.

## 6. Conclusions

A full 3-D CFD simulation of twin-screw pump has been carried out using structured moving numerical mesh with the conformal interface between the rotor domains. The cavitation intensity and distribution area were predicted based on the combination of VOF method and the Sauer-Scherr model. Through analysis and discussion, it can be concluded as follows:

- (1) If it appears, the cavitation will mainly happen in the area close to the suction port and will be distributed in the outward surfaces of rotors and clearances when the rotation speed is not too high. With the increase of rotation speeds beyond the current limit of pumps, the cavitation area will expand to the whole chamber along the rotor from suction to discharge.
- (2) The increase of rotation speed will enlarge the intensity of cavitation observably in screw pump. The increase of the discharge pressure at constant speed of rotation will increase the amplitude of volume fraction, while the average of volume fraction nearly remains the same.
- (3) The cavitation in screw pumps has many influence on the pump performance, which is manifested in larger pressure impact in screw rotors, increase of rotor torque and mass flowrate pulsation and larger power consumption.

The study of use of CFD for screw pumps provides better understanding of the internal flow field and cavitation characteristics, which provides a good basis for the next-step research on multiphase screw pump under different gas volume fraction (GVF).

**Acknowledgments:** This research was supported by the National Natural Science Foundation of China [grant number 51575069], State Key Program of National Natural Science of China [grant number 51635003] and Program of International S&T Corporation [grant number 2014DFA73030]. The project was performed at City University of London.

## References

- [1] Luca d'Agostino, Maria Salvetti, CISM International Centre for Mechanical Sciences: Fluid Dynamics of Cavitation and Cavitating Turbopumps, Udine: Springer-Verlag Wien, 2007. ISBN 978-3-211-76668-2.
- [2] Ruschel Andrej, Fluidodynamische Effekte in Schraubenspindelpumpen bei der Multiphasenförderung (Fluiddynamic effects in screw pumps at multiphase operation), Shaker Verlag GmbH, PhD thesis, Erlangen-Nürnberg University, 2014.
- [3] Brennen Christopher, Cavitation and Bubble Dynamics, New York: Oxford University Press, 1995. ISBN 0-19-509409-3.
- [4] Sham Rane, Ahmed Kovacevic, Nikola Stosic. Analytical Grid Generation for accurate representation of clearances in CFD for Screw Machines, in 9th International Conference on Compressors and their Systems, London, 2015.
- [5] STAR-CCM+ Version 9.06.009 Tutorial Guide.

- [6] Di Yan, Ahmed Kovacevic, Qian Tang, Sham Rane, Wenhua Zhang, Numerical Modelling of Twin-screw Pumps Based on Computational Fluid Dynamics, Proceedings of IMechE, Part C: Journal of Mechanical Engineering Science, vol. 0, no. 0, pp. 1-18, 2016.
- [7] Ahmed Kovacevic, Di Yan, Qian Tang, Sham Rane. Numerical Investigation of Twin-Screw Pump by Use of CFD, Proceeding of 13<sup>th</sup> Fluid Machinery Congress, Hague, 3-4 October 2016. ISBN 978-0-9956263-0-0
- [8] C.W Hirt, B.D Nichols, Volume of fluid (VOF) method for the dynamics of free boundaries, Journal of Computational Physics, vol. 39, no. 1, pp. 201-225, 1981.
- [9] I. Demirdžić, S. Muzaferija, Numerical Method for Coupled Fluid Flow, Heat Transfer and Stress Analysis Using Unstructured Moving Mesh with Cells of Arbitrary Topology, Computer Methods in Applied Mechanics and Engineering , vol. 125, no. 1-4, pp. 235-255, 1995.
- [10] Joel H. Ferziger, Milovan Peric, Computational Methods for Fluid Dynamics, 3rd Edition ed., Berlin Heidelberg: Springer-Verlag, 2002. ISBN 3-540-42074-6.
- [11] P. S. Epstein, M. S. Plesset. On the Stability of Gas Bubbles in Liquid-Gas Solutions, vol. 18, no. 11, pp. 1505-1509, 1950.
- [12] Sham Rane, Grid Generation and CFD analysis of variable Geometry Screw Machines, PhD thesis, City University London, London, 2015.
- [13] Rane S, Kovacevic A. Algebraic generation of single domain computational grid for twin screw machines. Part I. Implementation[J]. Advances in Engineering Software, vol. 107, pp.38-50, 2017.
- [14] Kovacevic A, Rane S. Algebraic generation of single domain computational grid for twin screw machines Part II – Validation[J]. Advances in Engineering Software, 2017.